20

FERMILAB
FEB 26 1997
LIBRARY

LAL/RT 97-01
February 1997

Laboratoire de l'Accélérateur Linéaire

BUNCH LENGTHENING AND CORRELATED ENERGY SPREADING IN ELECTRON STORAGE RINGS

LAL-RT-97-01

Fermilab Library
0 1160 0064678 0

J. Gao

Laboratoire de l'Accélérateur Linéaire,
IN2P3-CNRS et Université de Paris-Sud, F-91405 Orsay

NAME
REFUSED TO FERMILAB LIBRARY

Submitted to Particle Accelerators

U.E.R
de
l'Université Paris-Sud

Institut National
de Physique Nucléaire
et
de Physique des Particules

Bâtiment 200 - 91405 ORSAY Cedex

BUNCH LENGTHENING AND CORRELATED ENERGY SPREADING IN ELECTRON STORAGE RINGS

J. GAO
Laboratoire de L'Accélérateur Linéaire, IN2P3-CNRS
et Université de Paris-Sud,Centre d'Orsay,
F-91405 Orsay cedex, France

Abstract

A novel theory of bunch lengthening is established based on the equilibrium of synchrotron radiation damping and the excitations from synchrotron and collective quantum radiations. The mechanism of the bunch lengthening is found to be that the coupled synchrotron-collective quantum radiation excitation and the pure collective quantum radiation excitation move the zero current equilibrium bunch length to a new current dependent value. Analytical formulae are established to calculate the equilibrium bunch length and the correlated energy spread. Three current thresholds are given to distinguish the different bunch lengthening regions. Some experimental results are compared with those predicted by the theory and the comparison results are quite well. This theory will be useful in the design of high luminosity circular colliders and the damping rings for future linear colliders.

1 INTRODUCTION

The phenomenon of bunch lengthening as a single bunch effect in an electron storage ring was first observed in ACO [1] at Orsay and later in other machines. We summarize here the basic experimental observations [2] [3] [4]:

- The bunch lengthening is a single bunch effect which depends on the total electron population in the bunch and on the properties of the environments.
- The bunch lengthening is correlated to an energy spread increasing.
- There exist two current thresholds, $I_{b,1}$ and $I_{b,2}$ ($I_{b,1} < I_{b,2}$). Starting from $I_{b,1}$, appreciable bunch lengthening occurs. Above $I_{b,2}$, microwave instability appears accompanied with appreciable correlated energy spreading.
- At very low current ($I \ll I_{b,1}$) there is no appreciable bunch lengthening.
- At low current, $I < I_{b,1}$, it is possible to have a bunch shortening phenomenon.

The first empirical formula [1] found in ACO to describe the variation of the bunch duration (σ_τ) with respect to the average bunch current (I_b) and the beam energy (E), written

$$\sigma_\tau^2(\mathrm{ns}) = \sigma_{\tau 0}^2(\mathrm{ns})\left(1 + 2\times 10^{-3}\frac{I_b(\mathrm{mA})}{E^4(\mathrm{GeV})\sigma_\tau(\mathrm{ns})}\right) \tag{1}$$

had a great impact on the theories of longitudinal instabilities in electron storage rings established afterwards [5] [6]. The theories largely used to describe the phenomenon of bunch lengthening are potential well distortions and microwave instabilities. Potential well distortion theory was established to explain the bunch

lengthening without the correlation with the energy spread increasing, whereas the theory of microwave instability [7] was grafted from the theory of the instability in coasting proton beams [8].

In this paper we try to give a novel theory which describes the variations of the bunch length and the correlated energy spread with respect to the beam current covering the whole bunch current range.

In section 2, we review the synchrotron quantum radiation. The concept of collective quantum radiation is established in section 3, which is the physical base of this paper. In section 4, a novel bunch lengthening theory is established based on the *coupled synchrotron-collective quantum radiation excitation* and on the *pure collective quantum radiation excitations*, which move the zero current equilibrium bunch length and energy spread to new corresponding bunch current dependent values. In section 5, we give three current thresholds to describe the bunch lengthening effects in different current regions. Finally, in section 6, some experimental results are compared with the novel theory.

2 SYNCHROTRON QUANTUM RADIATION

It is well-known that in a circular accelerator [9] [10], the instantaneous synchrotron radiation power of an electron is

$$\mathcal{P}_p = \frac{e^2 c \gamma^4}{6\pi\epsilon_0 R^2} \tag{2}$$

and the energy loss per electron per turn for the isomagnetic case is

$$\mathcal{U}_0 = \frac{e^2 \beta^3 \gamma^4}{3\epsilon_0 R} \tag{3}$$

where R is the local bending radius and γ is the normalized energy. The total average power emitted by a bunch of N_e electrons is

$$\mathcal{P}_b = \frac{\mathcal{U}_0 N_e}{T_0} \tag{4}$$

where T_0 is the revolution period. The energy radiated per electron per unit frequency interval per turn is expressed as

$$\frac{dW_p}{d\omega} = \frac{\mathcal{U}_0}{\omega_c} S(\omega/\omega_c) \tag{5}$$

where

$$S(\omega/\omega_c) = \frac{9\sqrt{3}\omega}{8\pi\omega_c} \int_{\omega/\omega_c}^{\infty} K_{5/3}(\omega/\omega_c) d(\omega/\omega_c) \tag{6}$$

and

$$\omega_c = \frac{3\gamma^3 c}{2R} \tag{7}$$

The formulae given above are obtained with the assumption that the electron radiates energy in a continuous way, in reality however, energy is emitted in a discrete way, as "quanta" or photon, with an energy given by

$$u_p = \hbar\omega \tag{8}$$

where $\hbar = 1.05 \times 10^{-34} J \cdot sec$. Defining $n_p(u_p)$ as the number of the photons emitted per second per electron per energy interval, one has

$$n_p(u_p)\Delta u_p = \frac{c}{2\pi R\hbar\omega} \frac{dW_p}{d\omega} \Delta\omega \tag{9}$$

and

$$n_p(u_p) = \frac{\mathcal{P}_p}{u_c}\frac{S(u_p/u_c)}{(u_p/u_c)} \tag{10}$$

where

$$u_c = \hbar\omega_c = \frac{3\gamma^3\hbar c}{2R} \tag{11}$$

The total number of photons emitted per electron per second, $\mathcal{N}_p$, is then

$$\mathcal{N}_p = \int n_p(u_p)du_p = \frac{15\sqrt{3}\mathcal{P}_p}{8u_c} = \frac{5}{2\sqrt{3}}\frac{e^2\gamma}{4\pi\epsilon_0\hbar R} \tag{12}$$

From $n_p(u_p)$ one gets other statistical values, such as mean photon energy $< u_p >$ and mean square photon energy $< u_p^2 >$:

$$< u_p >= \frac{\int u_p n_p(u_p)du_p}{\mathcal{N}_p} = \frac{8}{15\sqrt{3}}u_c \tag{13}$$

$$< u_p^2 >= \frac{\int u_p^2 n_p(u_p)du_p}{\mathcal{N}_p} = \frac{11}{27}u_c^2 \tag{14}$$

3 COLLECTIVE QUANTUM RADIATION

In this section we will introduce the concept of *collective quantum radiation* which is necessary in treating the collective effects in a storage ring in a general way. It is well-known that a charged particle travelling inside a vacuum chamber will interact with its environments, such as the resistive wall beam pipe and the rf cavities, and thus lose its energy. It is usually convenient to use impedances [11] to describe the interaction between a charged particle and its environments. We define

$$Z_{||}(\omega) = \mathcal{R}_{||}(\omega) + i\mathcal{X}_{||}(\omega) \tag{15}$$

$$Z_{||}(\omega) = \frac{1}{c}\int_{-\infty}^{+\infty} \exp(i\omega z/c)W_{||}^{(0)}(z)ds \tag{16}$$

where $W_{||}^{(0)}(z)$ is the delta function longitudinal wake potential. If the wake potential is produced by a bunch of charged particles, one has

$$W_{||}(z) = \int_{-\infty}^{+\infty} \lambda(z-z')W_{||}^{(0)}(z')dz' \tag{17}$$

where $\lambda(z)$ is the longitudinal charge distribution, for example, for a bunch of unit charge and gaussian distribution, one has

$$\lambda(z) = \frac{c}{\sqrt{2\pi}\sigma_z}\exp(-z^2/2\sigma_z^2) \tag{18}$$

where σ_z is the r.m.s. bunch length. The loss factor of this bunch can be expressed as

$$\mathcal{K}_{||} = \frac{1}{\pi}\int_0^{\infty} \mathcal{R}_{||}(\omega)\tilde{\lambda}^2(\omega)d\omega \tag{19}$$

where

$$\tilde{\lambda}(\omega) = \frac{1}{2\pi c}\int_{-\infty}^{+\infty} \lambda(s)\exp(-i\omega s/c)ds \tag{20}$$

and for a gaussian distribution

$$\tilde{\lambda}(\omega) = \exp\left(-\frac{(\omega\sigma_z)^2}{2c^2}\right) \tag{21}$$

Here, we make some important definitions as follows

$$\mathcal{K}_{||}^{\text{tot}} = \frac{1}{\pi}\int_0^\infty \mathcal{R}_{||}^{\text{tot}}(\omega)\tilde{\lambda}^2(\omega)d\omega \tag{22}$$

$$\mathcal{K}_{||}^{r} = \frac{1}{\pi}\int_0^\infty \mathcal{R}_{||}^{r}(\omega)\tilde{\lambda}^2(\omega)d\omega \tag{23}$$

$$\mathcal{K}_{||}^{l} = \frac{1}{\pi}\int_0^\infty \mathcal{R}_{||}^{l}(\omega)\tilde{\lambda}^2(\omega)d\omega \tag{24}$$

where $\mathcal{K}_{||}^{\text{tot}}$ is the loss factor of the whole ring, $\mathcal{K}_{||}^{r}$ is the loss factor in the region where the design orbit trajectory has finite curvature, and $\mathcal{K}_{||}^{l}$ is the loss factor in the region where the design orbit trajectory is a straight line. Obviously, $\mathcal{K}_{||}^{\text{tot}} = \mathcal{K}_{||}^{r} + \mathcal{K}_{||}^{l}$. The three different regions are denoted by the upscripts tot, r, and l, respectively.

Some impedances of the beam environments in an electron storage ring, such as the resistive wall beam pipe and the accelerating rf cavities, can be calculated analytically. The impedance of a round resistive wall beam pipe of radius a per meter can be expressed as [12]

$$Z_{||}(\omega) = \frac{1}{2\pi a}\sqrt{\frac{Z_0\omega}{2\sigma c}}(1-i) \tag{25}$$

when $s \gg s_0 = (a^2/Z_0\sigma)^{1/3}$, where s is the distance between the exciting particle and the test particle, Z_0 is the free space impedance, and σ is the metal conductivity; at 300 K for copper, $\sigma = 5.9 \times 10^7\Omega^{-1}\text{m}^{-1}$, and for aluminum, $\sigma = 3.54 \times 10^7\Omega^{-1}\text{m}^{-1}$. The resistive wall loss factor with the pipe length of $2\pi R$ (isomagnetic lattice) is

$$\mathcal{K}_{||,\text{res.}}^{r} = \frac{cR}{2\pi a}\sqrt{\frac{Z_0}{2\sigma}}\frac{\Gamma(\frac{3}{4})}{\sigma_z^{3/2}} \tag{26}$$

with

$$\mathcal{R}_{||,\text{res.}}^{r}(\omega) = \frac{R}{a}\sqrt{\frac{Z_0\omega}{2\sigma c}} \tag{27}$$

The loss factor and the impedance of a cavity of length h and beam pipe radius a are [13] [14]

$$\mathcal{K}_{||,\text{cav.}} = \frac{1}{2\pi^2\epsilon_0 a}\left(\sqrt{\frac{h}{\sigma_z}} - 1\right) \tag{28}$$

$$\mathcal{R}_{||,\text{cav.}}(\omega) = \frac{Z_0}{2\pi a}\sqrt{\frac{hc}{\pi\omega}} \tag{29}$$

Since the energy loss of an electron bunch due to collective wake potentials is in the form of electromagnetic fields, in reality, the energy is emitted also in the form of "quanta" just like the synchrotron quantum radiation. By analogy, defining $n_w(u_w)$ as the number of photons emitted per second, per electron and per unit energy interval (since one cannot distinguish one electron from another in the bunch due to the synchrotron oscillation), one has

$$n_w(u_w)\Delta u_w = \frac{dW_w}{d\omega}\frac{1}{\hbar T_0\omega}\Delta\omega \tag{30}$$

where

$$\frac{dW_w}{d\omega} = \frac{e^2 N_e}{\pi}\mathcal{R}_{||}(\omega)\tilde{\lambda}^2(\omega) = e^2 N_e \mathcal{K}_{||} S_w(\omega) \tag{31}$$

with

$$S_w(\omega) = \frac{1}{\pi\mathcal{K}_{||}}\mathcal{R}_{||}(\omega)\tilde{\lambda}^2(\omega) \tag{32}$$

and

$$\int_0^\infty S_w(\omega)d\omega = 1 \tag{33}$$

The total number of photons emitted per electron per second, $\mathcal{N}_w$, is expressed then as

$$\mathcal{N}_w = \int n_w(u_\omega)du_w = \frac{e^2 N_e}{\pi T_0 \hbar}\Lambda \tag{34}$$

where

$$\Lambda = \int_0^\infty \frac{\mathcal{R}_{||}(\omega)}{\omega}\tilde{\lambda}^2(\omega)d\omega \tag{35}$$

For a pure resistive wall round pipe and a bunch of gaussian charge distribution, one gets

$$\Lambda^r_{\text{res.}} = \frac{\pi R}{2a\Gamma(3/4)}\sqrt{\frac{Z_0}{\sigma\sigma_z}} \tag{36}$$

$$\mathcal{N}^r_{w,\text{res.}} = \frac{e^2 N_e R}{2a\hbar T_0\Gamma(3/4)}\sqrt{\frac{Z_0}{\sigma\sigma_z}} \tag{37}$$

and

$$S^r_{w,\text{res.}}(\omega) = 2\left(\frac{\sigma_z}{c}\right)^{3/2}\frac{\sqrt{\omega}}{\Gamma(3/4)}\exp\left(-\left(\frac{\omega\sigma_z}{c}\right)^2\right) \tag{38}$$

The maximum of $S^r_{w,\text{res.}}(\omega)$ occurs at $\omega_m = c/2\sigma_z$ as shown in Fig. 1. For a bunch length $\sigma_z = 1$ cm, $f_m = \omega_m/2\pi = 2.387$ GHz, which is in the microwave region. To prevent this peaked em wave travelling inside the beam pipe, the pipe radius a should be chosen in the way that $\omega_{\text{cutoff}} = \nu_{01}c/a > \omega_m = c/2\sigma_z$. To compare the spectrum shown in Fig. 1 with that of the synchrotron radiation, normalizing $S^r_{w,\text{res.}}(\omega)$ by ω_c, we give a special example with $R = 1.7$ m, $\gamma = 1566$ and $\sigma_z = 1$ cm which is shown in Fig. 2. It is obvious that the collective radiation spectrum is relatively very narrow.

4 THEORY OF BUNCH LENGTHENING AND THE CORRELATED ENERGY SPREADING

From the experimental evidences shown in section 1, it is natural to think that the increased bunch length is simply a new equilibrium state away from the zero current bunch length. The mechanism to maintain this equilibrium is still the radiation damping and the quantum excitation. However, for the non-zero current case, the quantum excitations have to include the contribution from the collective quantum radiation discussed in the previous section. Having this physical picture in mind, we start now to see what happens when an additional stochastic quantum radiation is included, which is an independent random process with respect to the synchrotron quantum radiation.

The synchrotron oscillation in an electron storage ring without damping can be described by a simple oscillator:

$$\mathcal{E}(t) = \mathcal{A}\cos(\Omega_s t + \phi) \tag{39}$$

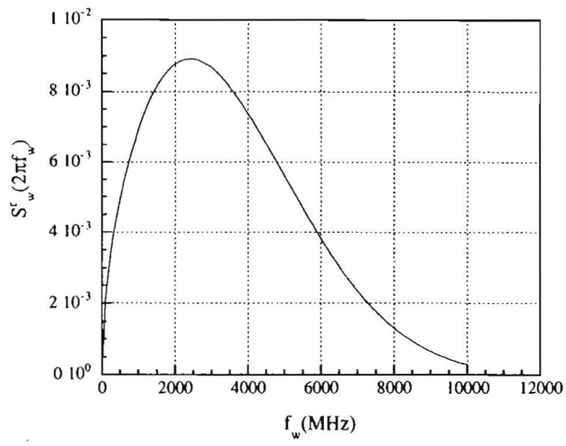

Figure 1: The collective quantum radiation spectrum with with $R = 1.7$ m, $\gamma = 1566$ and $\sigma_z = 1$ cm.

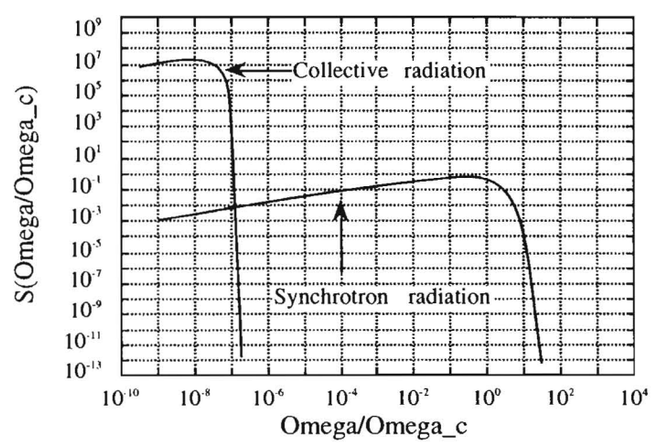

Figure 2: Comparison of the normalized collective quantum radiation spectrum with that of the synchrotron radiation with $R = 1.7$ m, $\gamma = 1566$ and $\sigma_z = 1$ cm.

$$\tau(t) = -\frac{\alpha}{E\Omega_s}\mathcal{A}\sin(\Omega_s t + \phi) \tag{40}$$

where $\mathcal{E}(t)$ and $\tau(t)$ are the energy and the position differences of an electron with respect to the synchronous electron, α is the momentum compaction factor, E is the electron energy, and Ω_s is the synchrotron oscillation angular frequency expressed as follows

$$\Omega_s = \left(\frac{ep\alpha\omega_{\text{rev.}}^2 V_{rf}\sin\phi_s}{2\pi E}\right)^{1/2} \tag{41}$$

where α is the momentum compaction factor, $\omega_{\text{rev.}}$ and ω_{rf} are the revolution and the rf angular frequencies, respectively, $p = \omega_{rf}/\omega_{\text{rev.}}$ is the harmonic number, $\phi_s = \cos^{-1}(\mathcal{U}_0/eV_{rf})$, and V_{rf} is the rf accelerating voltage. The invariant of the motion is given by:

$$\mathcal{A}^2 = \mathcal{E}(t)^2 + \left(\frac{E\Omega_s}{\alpha}\right)^2 \tau(t)^2 \tag{42}$$

If at times t_p and t_w two photons are emitted randomly and independently, one from the synchrotron quantum radiation and another from the collective quantum radiation, one has then

$$\mathcal{E}' = \mathcal{A}\cos(\Omega_s t + \phi) - u_p\cos(\Omega_s(t - t_p)) - u_w\cos(\Omega_s(t - t_w)) \tag{43}$$

and

$$\tau' = -\frac{\mathcal{A}\alpha}{\Omega_s E}\sin(\Omega_s t + \phi) + \frac{u_p\alpha}{\Omega_s E}\sin(\Omega_s(t - t_p)) + \frac{u_w\alpha}{\Omega_s E}\sin(\Omega_s(t - t_w)) \tag{44}$$

The increment in $\mathcal{A}^2$ is

$$\delta\mathcal{A}^2 = \mathcal{A}'^2 - \mathcal{A}^2$$

$$= u_p^2 + u_w^2 - 2\mathcal{A}u_p\cos(\Omega_s t_p + \phi) - 2\mathcal{A}u_w\cos(\Omega_s t_w + \phi) + 2u_p u_w\cos(\Omega_s(t_w - t_p)) \tag{45}$$

Since the t_p and t_w are completely unpredictable, and since we are interested only in the average effect, we calculate the average value of $\delta\mathcal{A}^2$ over one synchrotron oscillation period, T_s. It is found

$$< \delta\mathcal{A}^2 >= u_p^2 + u_w^2 - \mathcal{A}^2\frac{du_p}{dE} - \mathcal{A}^2\frac{du_w}{dE} + < 2u_w u_p\cos(\Omega_s(t_w - t_p)) >_{T_s} \tag{46}$$

where the notation $<>_{T_s}$ means the average over the period T_s.

If one estimates the average rate of change of $< \delta\mathcal{A}^2 >$ during one revolution period T_0, it is found that

$$\frac{d < \delta\mathcal{A}^2 >}{dt} =< \mathcal{N}_p < u_p^2 >> + \frac{\mathcal{U}_w^2}{T_0}$$

$$-\frac{\mathcal{A}^2}{T_0}\frac{d\mathcal{U}_p}{dE} - \frac{\mathcal{A}^2}{T_0}\frac{d\mathcal{U}_w}{dE} + \frac{2}{T_0}\sum_{i=1}^{N_w}\sum_{j=1}^{N_p} < u_w^i u_p^j\cos(\Omega_s(t_w^i - t_p^j)) >_{T_s} \tag{47}$$

where $\mathcal{U}_p$ and $\mathcal{U}_w$ are the total photon energies emitted from one electron during T_0, $N_w = \mathcal{N}_w T_0$ and $N_p = \mathcal{N}_p T_0$ are the numbers of photons emitted from one electron during T_0 due to the collective and synchrotron radiations.

For the equilibrium state, one has

$$\frac{d < \delta\mathcal{A}^2 >}{dt} = 0 \tag{48}$$

which leads to

$$< \mathcal{A}^2 >= \frac{\tau_{\varepsilon,p}\tau_{\varepsilon,w}}{2(\tau_{\varepsilon,p} + \tau_{\varepsilon,w})} < \mathcal{N}_p < u_p^2 >> (1+$$

$$\frac{2}{T_0 < \mathcal{N}_p < u_p^2 >>} \sum_{i=1}^{N_w} \sum_{j=1}^{N_p} < u_w^i u_p^j \cos(\Omega_s (t_w^i - t_p^j)) >_{T_s} + \frac{\mathcal{U}_w^2}{T_0 < \mathcal{N}_p < u_p^2 >>}) \quad (49)$$

where $\mathcal{U}_w = e^2 N_e K_{||}^{\text{tot}}$, $\tau_{\varepsilon,p} = 2T_0/\frac{d\mathcal{U}_p}{dE}$ and $\tau_{\varepsilon,w} = 2T_0/\frac{d\mathcal{U}_w}{dE}$ are the damping times from the synchrotron and the collective radiations, respectively (the later is usually very large, in the following it will be neglected). Consequently, the mean square equilibrium value of the energy deviation is

$$\mathcal{E}^2 = \frac{< \mathcal{A}^2 >}{2} \quad (50)$$

Till now, nothing has been said about the distribution function of the energy deviation. As we have described above, the energy oscillations are linear with respect to the energy deviation, and the total energy deviation is contributed by a large number of small statistically independent terms (except the second term in eq. 49). Therefore, according to the Central Limit Theorem of the probability theory, one knows that the resulting energy deviation distribution is gaussian (approximately, due to the second term in eq. 49), and that

$$\sigma_\varepsilon^2 = \mathcal{E}^2 =$$

$$\sigma_{\varepsilon_0}^2 \left(1 + \frac{2}{T_0 < \mathcal{N}_p < u_p^2 >>} \sum_{i=1}^{N_w} \sum_{j=1}^{N_p} < u_w^i u_p^j \cos(\Omega_s (t_w^i - t_p^j)) >_{T_s} + \frac{\mathcal{U}_w^2}{T_0 < \mathcal{N}_p < u_p^2 >>} \right) \quad (51)$$

where σ_{ε_0} is the zero current equilibrium energy spread.

A gaussian energy deviation distribution will result in a similar distribution for the time deviation τ, and one has therefore

$$\sigma_\tau^2 = \left(\frac{\alpha}{\Omega_s E} \right)^2 \sigma_\varepsilon^2$$

$$= \sigma_{\tau_0}^2 \left(1 + \frac{2}{T_0 < \mathcal{N}_p < u_p^2 >>} \sum_{i=1}^{N_w} \sum_{j=1}^{N_p} < u_w^i u_p^j \cos(\Omega_s (t_w^i - t_p^j)) >_{T_s} + \frac{\mathcal{U}_w^2}{T_0 < \mathcal{N}_p < u_p^2 >>} \right) \quad (52)$$

where σ_{τ_0} is the zero current equilibrium bunch duration. For an isomagnetic ring σ_{ε_0} and σ_{τ_0} can be expressed as

$$\sigma_{\varepsilon_0}^2 = C_q \frac{\gamma^2 E^2}{J_\epsilon R} \quad (53)$$

$$\sigma_{\tau_0}^2 = \left(\frac{\alpha}{\Omega_s} \right)^2 C_q \frac{\gamma^2}{J_\epsilon R} \quad (54)$$

where

$$J_\epsilon = 2 + \mathcal{D} \quad (55)$$

and

$$\mathcal{D} = \frac{\int_C \frac{D(z)}{R} (1/R^2 - 2k) ds}{\int_C \frac{1}{R^2} ds} \quad (56)$$

where $D(z)$ is the dispersion function, k is the focusing parameter defined as $kR = -(dB/dx)/B_0$, and $C_q = 55\hbar/32\sqrt{3}m_0 c = 3.84 \times 10^{-13}$ m (electron).

Eqs. 51 and 52 give the variation of the single bunch energy spread and the bunch duration with respect to the electron populations, and it is obvious that both quantities are correlated.

5 CURRENT THRESHOLDS

According to the theory established in section 4, one knows that $\sigma_\varepsilon^2/\sigma_{\varepsilon_0}^2$ and $\sigma_\tau^2/\sigma_{\tau_0}^2$ varying with the bunch population can be described by the same function expressed as follows

$$\left(\frac{\sigma_\iota}{\sigma_{\iota 0}}\right)^2 = 1 + \frac{2}{T_0 < \mathcal{N}_p < u_p^2 >>} \sum_{i=1}^{N_w} \sum_{j=1}^{N_p} < u_w^i u_p^j \cos(\Psi_j^i) >_{T_s} + \frac{\mathcal{U}_w^2}{T_0 < \mathcal{N}_p < u_p^2 >>} \tag{57}$$

where σ_ι represents either the bunch length or the energy spread, and $\Psi_j^i = \Omega_s(t_w^i - t_p^j)$. In this section we will give some current thresholds to distinguish different behaviours of the bunch lengthening with respect to the bunch current, and the term "current threshold" in this section is not connected with any fast longitudinal instabilities.

5.1 The First Current Threshold

When N_e is very small, the total number of photons from the collective radiation emitted during one synchrotron period, N_w, is much less than that of the synchrotron radiation, N_p. Consequently, Ψ can have almost any possible value and the second term in eq. 57 will be zero. However, when $N_w \geq N_p$, the phase Ψ will be *locked* to almost zero and the *coupling* between the synchrotron radiation and the collective radiation is established and maintained. The time duration for the phase lock process to start and finish is about one synchrotron oscillation period. Since only the photons emitted by the synchrotron and the collective radiations in the regions where the local design orbit trajectory has finite curvatures can be possibly emitted simultaneously, by setting

$$< \mathcal{N}_p >= \mathcal{N}_w^r \tag{58}$$

one gets the first threshold for the bunch population

$$N_e^{th1} = \frac{5\pi\gamma Z_0}{4\sqrt{3}\Lambda^r} \tag{59}$$

and the first threshold for an average single bunch current

$$I_b^{th1} = \frac{eN_e^{th1}c}{2\pi R_{av}} \tag{60}$$

where $R_{av} = cT_0/2\pi$. If the vacuum chamber in this region is a round pipe, by putting eq. 36 into eq. 59, one gets

$$N_{e,R}^{th1} = \frac{5\gamma a\Gamma(3/4)}{2\sqrt{3}R}\sqrt{\sigma\sigma_z Z_0} \tag{61}$$

and

$$I_{b,R}^{th1} = \frac{5\gamma aec\Gamma(3/4)}{4\pi\sqrt{3}RR_{av}}\sqrt{\sigma\sigma_z Z_0} \tag{62}$$

When $I_b \ll I_b^{th1}$, there will be no appreciable bunch lengthening and correlated energy spreading (the third term in eq. 57 is neglected). When $I_b \sim I_b^{th1}$, however, it will be possible to have some bunch lengthening or shortening depending on the sign of the second term which has the *stochastic properties*. Anyway, in the region $I_b \leq I_b^{th1}$, the bunch length is still dominated by the synchrotron quantum excitation.

5.2 The Second Current Threshold

When $N_e \geq N_e^{th1}$ the coupled radiation occurs in the region where the local designed orbit curvature is not infinite and eq. 57 can be simplified as

$$\left(\frac{\sigma_\iota}{\sigma_{\iota 0}}\right)^2 = 1 + \frac{2 < \mathcal{N}_p < u_p >> e^2 N_e \mathcal{K}_{||}^r}{< \mathcal{N}_p < u_p^2 >>} + \frac{\mathcal{U}_w^2}{T_0 < \mathcal{N}_p < u_p^2 >>} \tag{63}$$

where $\mathcal{K}_{||}^r$ is the loss factor in the region where R is finite. When the second term in eq. 63 is equal to one, it begins to dominate the bunch lengthening. One gets therefore

$$N_e^{th2} = \frac{< \mathcal{N}_p < u_p^2 >>}{2 < \mathcal{N}_p < u_p >> e^2 \mathcal{K}_{||}^r} \tag{64}$$

For an isomagnetic ring

$$\left(\frac{\sigma_\iota}{\sigma_{\iota 0}}\right)^2 = 1 + \frac{96 e^2 N_e \mathcal{K}_{||}^r R}{55\sqrt{3}\hbar c \gamma^3} + \frac{144 \epsilon_0 (e R N_e \mathcal{K}_{||}^{\text{tot}})^2}{55\sqrt{3}\hbar c \gamma^7} \tag{65}$$

$$N_e^{th2} = \frac{55\sqrt{3}\hbar c \gamma^3}{96 e^2 R \mathcal{K}_{||}^r} \tag{66}$$

and

$$I_b^{th2} = \frac{e N_e^{th2} c}{2\pi R_{av}} \tag{67}$$

5.3 The Third Current Threshold

As N_e increases, the third term is no longer negligible, and when the third term in eq. 63 is equal to the second term, the third term, or the collective quantum radiation, begins to dominate the bunch lengthening. One has then

$$N_e^{th3} = \frac{2 < \mathcal{N}_p < u_p >> T_0 \mathcal{K}_{||}^r}{e^2 (\mathcal{K}_{||}^{\text{tot}})^2} \tag{68}$$

For an isomagnetic ring, one gets

$$N_e^{th3} = \frac{2\gamma^4 \mathcal{K}_{||}^r}{3\epsilon_0 R (\mathcal{K}_{||}^{\text{tot}})^2} \tag{69}$$

$$I_b^{th3} = \frac{e N_e^{th3} c}{2\pi R_{av}} \tag{70}$$

5.4 Discussion

We summarize first what we have obtained in this section. When $N_e < N_e^{th1}$ there is almost no bunch lengthening nor additional correlated energy spreading. When $N_e^{th2} \ll N_e < N_e^{th3}$

$$\frac{\sigma_\iota^2}{\sigma_{\iota 0}^2} = \frac{96 e^2 N_e \mathcal{K}_{||}^r R}{55\sqrt{3}\hbar c \gamma^3} \tag{71}$$

and when $N_e \gg N_e^{th3}$

$$\frac{\sigma_\iota^2}{\sigma_{\iota 0}^2} = \frac{144 \epsilon_0 (e R N_e \mathcal{K}_{||}^{\text{tot}})^2}{55\sqrt{3}\hbar c \gamma^7} \tag{72}$$

Since $\mathcal{K}_{||}^{r}$ and $\mathcal{K}_{||}^{tot}$ are functions of σ_z, one can write

$$\mathcal{K}_{||}^{r} = \mathcal{K}_{||,0}^{r}\left(\frac{\sigma_{z0}}{\sigma_z}\right)^{\varpi} \tag{73}$$

and

$$\mathcal{K}_{||}^{tot} = \mathcal{K}_{||,0}^{tot}\left(\frac{\sigma_{z0}}{\sigma_z}\right)^{\varsigma} \tag{74}$$

where $\mathcal{K}_{||,0}^{r}$ and $\mathcal{K}_{||,0}^{tot}$ are the loss factors at $\sigma_z = \sigma_{z0}$, and σ_{z0} is the natural bunch length. Consequently, eqs. 71 and 72 can be rewritten as

$$R^{\dagger} = \frac{\sigma_z}{\sigma_{z0}} = \left(\frac{96e^2 N_e \mathcal{K}_{||,0}^{r} R}{55\sqrt{3}\hbar c\gamma^3}\right)^{\frac{1}{2+\varpi}} \tag{75}$$

and

$$R^{\ddagger} = \frac{\sigma_z}{\sigma_{z0}} = \left(\frac{144\epsilon_0 (eRN_e\mathcal{K}_{||,0}^{tot})^2}{55\sqrt{3}\hbar c\gamma^7}\right)^{\frac{1}{2+2\varsigma}} \tag{76}$$

When $\mathcal{K}_{||}^{r}$ comes mainly from resistive wall, $\varpi = 3/2$, and if SPEAR scaling law [4] is used, $\varsigma \approx 1.21$. The scaling laws are obtained for the coupled radiation dominated region as

$$R^{\dagger} \propto \left(\frac{I_b R R_{av} \mathcal{K}_{||,0}^{r}}{\gamma^3}\right)^{\frac{1}{3.5}} \tag{77}$$

and for the collective radiation dominated region as

$$R^{\ddagger} \propto \left(\frac{I_b^2 R^2 R_{av}^2 (\mathcal{K}_{||,0}^{tot})^2}{\gamma^7}\right)^{\frac{1}{4.42}} \tag{78}$$

where $I_b = eN_e c/2\pi R_{av}$.

For the general case, however, eq. 65 can be simplified as

$$\mathbf{R}^2 = 1 + \frac{C_1 I_b R_{av} R \mathcal{K}_{||,0}^{r}}{\gamma^3 \mathbf{R}^{1.5}} + \frac{C_2 (R_{av} R I_b \mathcal{K}_{||,0}^{tot})^2}{\gamma^7 \mathbf{R}^{2.42}} \tag{79}$$

where $\mathbf{R} = \sigma_z/\sigma_{z0}$, C_1 and C_2 are expressed as follows

$$C_1 = \frac{192\pi e}{55\sqrt{3}\hbar c^2} \tag{80}$$

$$C_2 = \frac{576\pi^2\epsilon_0}{55\sqrt{3}\hbar c^3} \tag{81}$$

Till now, the novel theory developed in this paper has said nothing about the effect of the potential well distortion. It is interesting to recall the corresponding general formula from the potential well distortion theory, which is expressed as follows [5] [6]

$$\mathbf{R}^2 = 1 + \frac{C_0 I_b}{\gamma^3 \mathbf{R}} \tag{82}$$

where C_0 is proportional to $\frac{1}{\alpha}$ and a function of the lattice parameters and the longitudinal impedance of the machine [5] [6]. Including the potential well distortion effect, eq. 79 becomes

$$\mathbf{R}^2 = 1 + \frac{C_0 I_b}{\gamma^3 \mathbf{R}} + \frac{C_1 I_b R_{av} R \mathcal{K}_{||,0}^{r}}{\gamma^3 \mathbf{R}^{1.5}} + \frac{C_2 (R_{av} R I_b \mathcal{K}_{||,0}^{tot})^2}{\gamma^7 \mathbf{R}^{2.42}} \tag{83}$$

Machine name	E (GeV)	γ	R (m)	R_{av} (m)	σ_{z0} (cm)	$\mathcal{K}_{\|\|,0}^{tot}$ (V/pC)
ACO	0.238	467	1.11	3.41	21.7	0.525
KEK-PF	2.5	4892	8.66	29.8	1.47	3.7
KEK-PF	1.8	3523	8.66	29.8	1.1	5.4
BEPC	1.3	2544	10.345	38.2	1	9.6
BEPC	2.02	3943	10.345	38.2	2	3.82
SPEAR	1.5	2935	12.7	37.3	-	5.2
Super-ACO	0.8	1566	1.7	11.5	2.4	3.1

Table 1: The machine parameters and the total loss factors.

What should be pointed out is that C_1 and C_2 are two positive numbers, however, C_0 can be negative if the momentum compaction factor, α, is negative. It is clear that by choosing a negative momentum compaction factor the bunch lengthening effect can be moderated as suggested by Fang et al. [15] and experimentally proved by the Super-ACO group [16]. Since the potential well distortion does not increase the energy spread, eq. 65 can always be used to calculate energy spreading. It is evident that for the negative α case the energy spreading is more important than that of the positive α ($|\alpha|$ is the same for both cases) as evidenced in ref. 16, since the bunch length is shorter and the loss factor is larger for $\alpha < 0$.

In fact, when $\alpha > 0$, the second and the third terms in eq. 83 can be combined (since they follow almost the same scaling law), and in the following section we will keep using eq. 79 to fit the experimental results.

Finally, if in a storage ring there are other insertion components, such as wigglers which give additional local design orbit curvature radii, one has to take into account the coupled radiations in these components as well.

6 COMPARISON WITH EXPERIMENTAL RESULTS

In this section we use the novel theory developed above to explain the experimental bunch lengthening measurement results in different storage rings, such as ACO, KEK Photon Factory (KEK-PF), BEPC, SPEAR and Super-ACO. The corresponding machine parameters are shown in table 1. Since there are few informations about the loss factors, $\mathcal{K}_{||}^{r}$ and the $\mathcal{K}_{||}^{tot}$, for these machines, we shall fit the experimental bunch lengthening curves by eq. 79 and extract the information on the total loss factor at a given bunch length for the corresponding machines.

Firstly, we look at the ACO storage ring [17]. Using eqs. 79 and 82 one fits the experimental results as shown in Fig. 3, where the dark line corresponds to the novel theory (the same for all the following figures) which gives the total loss factor $\mathcal{K}_{||,0}^{tot} = 0.525$ V/pC at $\sigma_{z0} = 21.7$ cm.

Secondly, we look at KEK photon factory storage ring [18]. The experimental results are fitted by eqs. 79 and 82, and shown in Fig. 4. In ref. 16, it is stated that when the experimental results deviate from the curve predicted by the potential well distortion theory, the microwave instability occurs. According to the novel theory, however, the deviation is due to the additional effect from the pure collective radiation excitation (the third term in eq. 79). Fig. 5 illustrates two extreme cases. The curves denoted "no second term" and "no third term" are the results when one turns off either the second or the third terms in eq. 79, respectively. Figs. 6 and 7 give the similar results at a different beam energy. The total loss factor $\mathcal{K}_{||,0}^{tot} = 5.4$

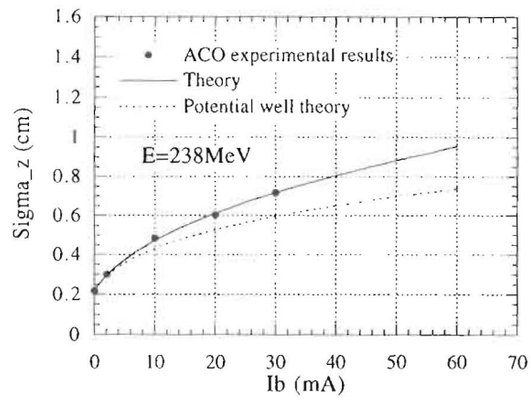

Figure 3: Comparison between ACO experimental results, the theoretical results and the potential well distortion theory predictions at 238 MeV with σ_{z0}=21.7 cm. The continuous and the dotted lines are the fitted curves of the novel and the potential well distortion theories, respectively. The dark points are the ACO experimental results.

V/pC at $\sigma_{z0} = 1.1$ cm is obtained from the two experimental results at different energies.

Thirdly, we look at BEPC (Beijing Electron Positron Collider) [19]. Fig. 8 shows the comparison results between the novel theory and the potential well theory. Fig. 9 shows the consequences when the second and the third terms in eq. 79 are switched off alternatively. Fig. 10 gives the similar comparison results at a different beam energy. Both experimental results lead to $\mathcal{K}_{||,0}^{tot} = 9$ V/pC at $\sigma_{z0} = 1$ cm.

Fourthly, the comparison results of SPEAR storage ring [20] are shown in Figs. 11 and 12.

Finally, Super-ACO [16] is considered and the comparison results are shown in Fig. 13. The total loss factor of the machine at $\sigma_z = 3$ cm is calculated as 2.22 V/pC by using TBCI [21], and the $\mathcal{K}_{||,0}^{tot}$ obtained from the experimental bunch lengthening curve is 2.38 V/pC for the same bunch length ($\mathcal{K}_{||,0}^{tot} = 3.1$ V/pC at $\sigma_{z0} = 2.4$ cm). What should be mentioned is that the experimental results shown in Fig. 13 correspond to the case of positive momentum compaction factor $\alpha = 0.0148$. If the momentum compaction factor $\alpha < 0$ (Super-ACO [16]), the potential well distortion effect should give bunch shortening. The combination with the present quantum excitation effect may give less bunch lengthening, however, the negative momentum compaction factor could not moderate the energy spread which is not affected by the potential well distortion. In consequence, as explained at the end of the last section, for the same $|\alpha|$, the energy spread is more important for the negative α case than that of the positive α case.

To summarize, in the last column of table 1 we give the total loss factors for the different machines found from the fitted curves at corresponding zero current equilibrium bunch lengths.

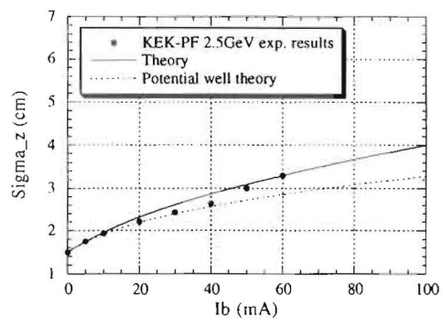

Figure 4: Comparison between KEK Photon Factory experimental results, the theoretical results and the potential well distortion theory predictions at 2.5 GeV with σ_{z0}=1.5 cm. The continuous and the dotted lines are the fitted curves of the novel and the potential well distortion theories, respectively. The dark points are the KEK-PF 2.5 GeV experimental results.

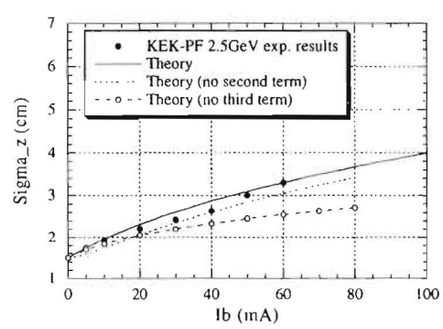

Figure 5: Comparison between KEK Photon Factory experimental results and the theoretical results at 2.5 GeV with σ_{z0}=1.5 cm. The continuous line is the fitted curve of the novel theory. The dotted and the circle-dotted lines are the fitted curves without the second or the third terms in eq. 79, respectively. The dark points are the KEK-PF 2.5 GeV experimental results.

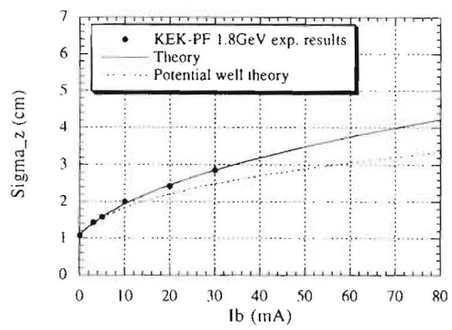

Figure 6: Comparison between KEK Photon Factory experimental results, the theoretical results and the potential well distortion theory predictions at 1.8 GeV with σ_{z0}=1.1 cm. The continuous and the dotted lines are the fitted curves of the novel and the potential well distortion theories, respectively. The dark points are the KEK-PF 1.8 GeV experimental results.

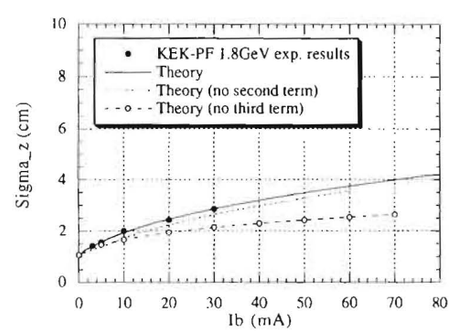

Figure 7: Comparison between KEK Photon Factory experimental results and the theoretical results at 1.8 GeV with σ_{z0}=1.1 cm. The continuous line is the fitted curve of the novel theory. The dotted and the circle-dotted lines are the fitted curves without the second or the third terms in eq. 79, respectively. The dark points are the KEK-PF 1.8 GeV experimental results.

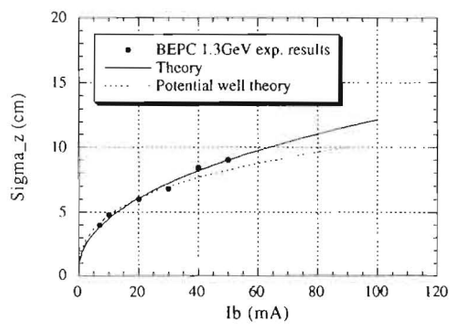

Figure 8: Comparison between BEPC experimental results, the theoretical results and the potential well distortion theory predictions at 1.3 GeV with σ_{z0}=1. cm. The continuous and the dotted lines are the fitted curves of the novel and the potential well distortion theories, respectively. The dark points are the BEPC 1.3 GeV experimental results.

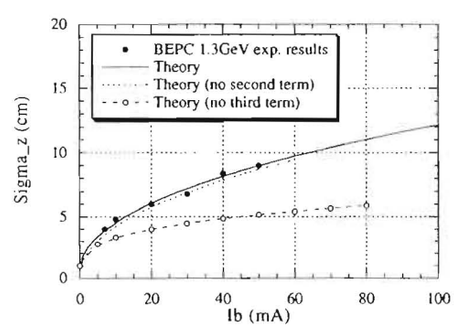

Figure 9: Comparison between BEPC experimental results and the theoretical results at 1.3 GeV with σ_{z0}=1. cm. The continuous line is the fitted curve of the novel theory. The dotted and the circle-dotted lines are the fitted curves without the second or the third terms in eq. 79, respectively. The dark points are the BEPC 1.3 GeV experimental results.

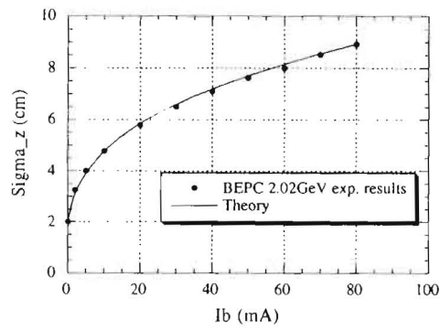

Figure 10: Comparison between BEPC experimental results and the theoretical results at 2.02 GeV with σ_{z0}=2 cm. The continuous line is the fitted curve of the novel theory. The dark points are the BEPC 2.02 GeV experimental results.

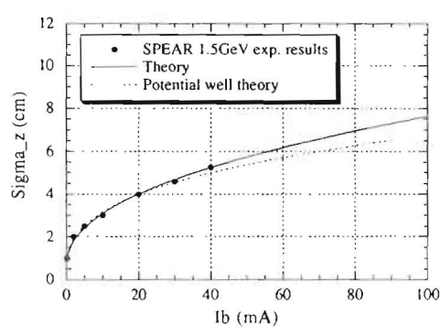

Figure 11: Comparison between SPEAR experimental results, the theoretical results and the potential well predictions at 1.5 GeV. The continuous and the dotted lines are the fitted curves of the novel and the potential well distortion theories, respectively. The dark points are the SPEAR 1.5 GeV experimental results.

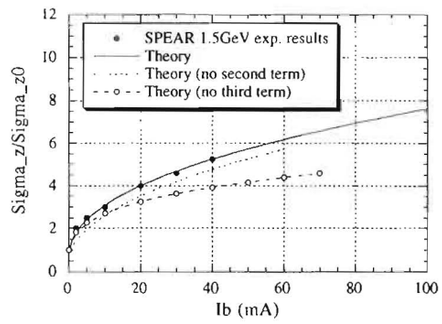

Figure 12: Comparison between SPEAR experimental results and the theoretical results at 1.5 GeV. The continuous line is the fitted curve of the novel theory. The dotted and the circle-dotted lines are the fitted curves without the second or the third terms in eq. 79, respectively. The dark points are the SPEAR 1.5 GeV experimental results.

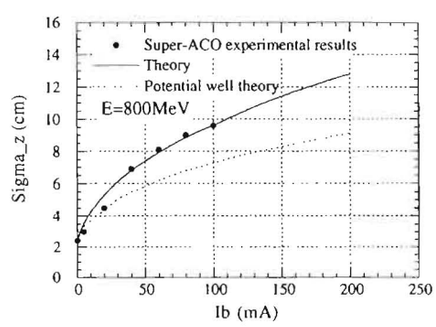

Figure 13: Comparison between Super-ACO experimental results, the theoretical results and the potential well distortion theory predictions at 800 MeV with σ_{z0}=2.4 cm. The continuous and the dotted lines are the fitted curves of the novel and the potential well distortion theories, respectively. The dark points are the Super-ACO 800 MeV experimental results.

7 CONCLUSION

Based on the concept of coupled synchrotron-collective quantum radiation excitation and the collective radiation excitation, a novel theory of bunch lengthening and the correlated energy spreading is established. It is demonstrated that the longitudinal loss factors (resistive part impedances of the machine) increase the bunch length and the energy spread. Some comparisons between experimental and theoretical results are made and the agreements are quite well. The theory developed in this paper will be useful in the design of high luminosity circular colliders and the damping rings for future linear colliders.

8 ACKNOWLEDGEMENTS

I would like to thank J. Le Duff for useful discussions, critical comments and numerous corrections on the manuscript.

References

[1] R. Belbeoch, M. Bergher, J. Le Duff, M.P. Level, P. Marin, Ch. Nguyen Ngoc, M.Sommer and H. Zyngier, "Recent experiments with ACO, in Proceedings of the national conference on particle accelerators", No. 1 (Moscow, 1968) p. 129 (in Russian).

[2] J. Le Duff, "Current and current limitations in existing electron storage rings", *Nucl. Instr. and Meth.* **A239** (1985) p.83.

[3] J. Gareyte" Experimental observations of electron beam instabilities in storage rings", *Nucl. Instr. and Meth.* **A239** (1985) p.72.

[4] P.B. Wilson, R. Servranckx, A.P. Sabersky, J. Gareyte, G.E. Fischer, A.W. Chao, and M.H.R. Donald, "Bunch lengthening and related effects in SPEAR II", *IEEE Trans. on Nucl. Sci.* **NS-24** (1977) p. 1211.

[5] C. Pellegrini and A.M. Sessler, "The equilibrium length of high-current bunches in electron storage rings", *Nuovo Cimento*, **3A** (1971) p. 116.

[6] J. Haissinski, "Exact longitudinal equilibrium distribution of stored electrons in the presence of self-fields", *Nuovo Cimento*, **18B** (1973) p. 72.

[7] D. Boussard, CERN LabII/RF/int./75-2 (1975).

[8] E. Keil and W. Schnell, CERN Int. Rep. ISR-TH-RF/69-48 (1969).

[9] M. Sands, "The physics of electron storage rings, an introduction" SLAC-121 (1970).

[10] B.P. Walker, "Synchrotron radiation" and "Radiation Damping", CERN 94-01 (1994) p. 437 and p. 461.

[11] P. Wilson, "Introduction to wakefields and wake potentials", SLAC-PUB-4547 (1989).

[12] O. Henry and O. Napoly, "The resistive-pipe wake potentials for short bunches", *Particle Accelerators*, **35** (1991) p. 235.

[13] A.V. Novokhatski, "One the estimation of the wake potential for an ultrarelativistic charge in an accelerating structure", Preprint 88-39, INP, Novosibirsk, Russia.

[14] G. Dôme, *IEEE, Trans. on Nucl. Sci.* **NS-32** (1985) p. 2531.

[15] S.X. Fang, et al. "Microwave instabilities in electron rings with negative momentum compaction factor", KEK Preprint 94-190 (1995).

[16] A. Nadji, et al., "Experiments with low and negative momentum compaction factor with Super-ACO", Proceedings of EPAC96, Barcelona (1996) p. 676.

[17] Le groupe de l'anneau de collisions d'Orsay, "Allongement des paquets dans ACO", Rapport technique 34-69, Orsay, le 14 novembre (1969).

[18] N. Nakamura, S. Sakanaka, K. Haga, M. Izawa, and T. Katsura, "Collective effects in single bunch mode at the photon factory storage ring", Proceedings of PAC91, San Francisco, CA (1991) p. 440.

[19] Z. Guo, et al., "Bunch lengthening study in BEPC", Proceedings of PAC95, Dallas TX (1995) p. 2955.

[20] SPEAR Group, "SPEAR II performance", *IEEE Trans. on Nucl. Sci.* **NS-22** (1975) p. 1366.

[21] P. Brunelle, "Etude théorique et expérimentale des faisceaux dans l'anneau VUV Super-ACO", thèse, 1990.